

## Analysis of Missed Summer Severe Rainfall Forecasts

ZUOHAO CAO

*Environment and Climate Change Canada, Toronto, Ontario, Canada*

DA-LIN ZHANG

*Department of Atmospheric and Oceanic Science, University of Maryland, College Park, College Park, Maryland*

(Manuscript received 11 September 2015, in final form 22 December 2015)

### ABSTRACT

Despite considerable progress in mesoscale numerical weather prediction (NWP), the ability to predict summer severe rainfall (SSR) in terms of amount, location, and timing remains very limited because of its association with convective or mesoscale phenomena. In this study, two representative missed SSR events that occurred in the highly populated Great Lakes regions are analyzed within the context of moisture availability, convective instability, and lifting mechanism in order to help identify the possible causes of these events and improve SSR forecasts/nowcasts. Results reveal the following limitations of the Canadian regional NWP model in predicting SSR events: 1) the model-predicted rainfall is phase shifted to an undesired location that is likely caused by the model initial condition errors, and 2) the model is unable to resolve the echo-training process because of the weakness of the parameterized convection and/or coarse resolutions. These limitations are related to the ensuing model-predicted features: 1) vertical motion in the areas of SSR occurrence is unfavorable for triggering parameterized convection and grid-scale condensation; 2) convective available potential energy is lacking for initial model spinup and later for elevating latent heating to higher levels through parameterized convection, giving rise to less precipitation; and 3) the conversion of water vapor into cloud water at the upper and middle levels is underpredicted. Recommendations for future improvements are discussed.

### 1. Introduction

Summer severe rainfall<sup>1</sup> (SSR) is often convective in nature and associated with mesoscale phenomena (e.g., Fritsch and Heideman 1989; Olson et al. 1995), and it is therefore difficult to predict in terms of the precipitation amount, location, and timing (e.g., Olson et al. 1995; Applequist et al. 2002; Fritsch and Carbone 2004). Development of SSR can be attributed to three major forcings (e.g., Bennett et al. 2006; Lopez 2007; Marsham et al. 2011): upper-level forcing, boundary layer forcing, and secondary generation formed through

the interaction of outflow from convective clouds with the surrounding environmental air. Despite considerable research carried out in the past decades (e.g., Maddox et al. 1979; Maddox 1980; Corfidi et al. 1996; Corfidi 2003; Weckwerth and Parsons 2006; Browning et al. 2007; Wulfmeyer et al. 2008; Schumacher and Johnson 2006; Gallus et al. 2008; Lombardo and Colle 2010; Jessup and Colucci 2012), including some incremental improvements that have been made in severe precipitation forecast accuracy (e.g., Sukovich et al. 2014), SSR still remains one of the least understood meteorological phenomena in the scientific and operational communities because of its involvement of multiscale dynamic and thermodynamic processes (e.g., Fritsch and Carbone 2004; Sukovich et al. 2014).

To date, operational meteorologists rely on the following three major techniques to forecast SSR events: 1) conceptual models (partially derived from pattern recognition), 2) numerical weather prediction (NWP) models, and 3) persistence nowcasts using observed precipitation amount and phase from approaching weather

---

<sup>1</sup> As defined by the OSPC, an SSR event is considered to occur when its rainfall rate exceeds 50 mm day<sup>-1</sup> or 75 mm in 48 h in Ontario.

---

*Corresponding author address:* Dr. Zuohao Cao, Meteorological Research Division, Environment and Climate Change Canada, 4905 Dufferin St., Toronto ON M3H 5T4, Canada.  
E-mail: zuohao.cao@canada.ca

systems (e.g., extrapolating radar echoes in time). The conceptual models of precipitation systems have been used for operational weather forecasts (e.g., [Browning 1986](#)). To consider regional weather and local effects, forecasters often need to develop their own conceptual models to support their hypotheses (e.g., [Whittier et al. 2004](#)). These conceptual models are usually formed through a mixture of theory, experience, and climatology (e.g., [Gordon and Albert 2012](#)). The conceptual models at their very best are a summary of past forecast experiences, which need to be updated in order to make more accurate predictions for precipitating systems and their associated severe events [e.g., Cooperative Institute for Precipitation Systems (CIPS) available online at <http://www.eas.slu.edu/CIPS/ANALOG/analog.php>; [Gravelle et al. \(2009\)](#)]. The NWP model-based precipitation forecasts often show errors in amount, location, type, and timing. These errors are mainly due to 1) the lack of sufficient observations in both space and time, as well as the limited use of observations; 2) missing or inadequate inclusion of physical processes in NWP models; and 3) our limited understanding of atmospheric physical processes ([Fritsch and Carbone 2004](#)). As for the persistence nowcast approaches, most, if not all, of them only consider the “advective” effect and have little to do with the “generation” of any new precipitation systems and the “dissipation” of any existing ones (e.g., [Germann and Zawadzki 2002](#)).

Analyses of observations during the last two decades over Ontario, Canada, indicate a substantial increase in the frequency of SSR events (e.g., [Cao and Ma 2009b](#); [Cao 2008](#)). The SSR events have significant impacts on Canadian society and the nation’s economy, especially in highly populated areas such as southern Ontario (e.g., [Cao et al. 2004](#)). However, most of these events have proven difficult to predict accurately in terms of their amount, location, and timing, and some of them are completely missed. In this study, we examine two representative missed SSR events (associated with three cyclones, and a quasi-stationary low pressure system) that were identified with inputs from a senior meteorologist (G. Robinson 2014, personal communication) of the Ontario Storm Prediction Center (OSPC) of Environment and Climate Change Canada. The two SSR events occurred in Ottawa on 24 July 2009, and Hamilton on 26 July 2009, hereafter referred to as Ottawa–24 July, and Hamilton–26 July, respectively. Through examining these SSR events that were missed by both human forecasters and the operational NWP models [e.g., Global Environmental Multiscale (GEM) regional model; [Côte et al. 1998](#)], we wish to 1) assess the model ability in forecasting SSR events and 2) provide evidence for endorsements on continuously improving

NWP model initial conditions and simulating SSR events using cloud-permitting NWP models. To the best of our knowledge, these efforts are relatively new since we are examining SSR events that were missed operationally whereas most of the published case studies (if not all) look at “successful” events.

The next section describes the data and methodology used in this study. [Sections 3 and 4](#) present analyses of the two SSR events. Concluding remarks and recommendations are given in the final section.

## 2. Data and methodology

Datasets used in this study include, but are not limited to, 1) the hourly operational GEM regional model forecast data with a 15-km grid spacing and 58 vertical levels ([Côte et al. 1998](#)), archived at the Canadian Meteorological Centre (CMC). Fields extracted from the GEM regional model 0000 UTC run include mean sea level pressure (MSLP), geopotential height, temperature, moisture, wind, rainfall (accumulation and rate), precipitable water, cloud area coverage, and convective available potential energy (CAPE); 2) the 3-hourly North American Regional Reanalysis (NARR) data with a grid spacing of 32 km and 29 constant pressure levels that are archived at the National Centers for Environmental Prediction (NCEP) ([Mesinger et al. 2006](#)); 3) the daily rain gauge data plus a small amount of the hourly rainfall data, obtained from the national climate center and/or the [Ontario Climate Center \(2005\)](#); 4) radar-estimated rainfall accumulation and rainfall rates at 10-min intervals obtained from the [Canadian National Radar Network \(2014\)](#), covering areas mainly along the U.S.–Canada border; and 5) the observed soundings obtained from the [University of Wyoming \(2014\)](#).

To verify rainfall forecasts and analyze synoptic environments, moisture variability, atmospheric instability, and lifting mechanisms (e.g., [Doswell et al. 1996](#)), we employ the following methodologies.

- 1) The GEM regional model predicted rainfall is verified against rain gauge observations, extracted from the Canada Climate Center’s archived dataset using spreadsheet software, and radar observations, obtained from the Canadian radar network data using the Unified Radar Processor (URP) software. In this study, we use a threshold value of 24-h accumulated precipitation of 50 mm or more to define an SSR event. For a forecast at a given location, if the model-predicted 24-h accumulated rainfall equals or exceeds the threshold, there will be a hit; otherwise, there will be a miss. On the other hand, if the model-predicted 24-h accumulated rainfall meets this

threshold but observed rainfall is not severe, a false alarm results. In this study, we are interested in rainfall forecasts at specific locations such as Ottawa and Hamilton; in such small areas, there are some but not many ground-truth surface observations available. As a result, we are unable to compute a threat score or bias score because the statistics required for these calculations cannot properly be met.

- 2) Synoptic environments associated with the SSR are analyzed by comparing the GEM regional model forecast and the NARR fields such as MSLP and geopotential height.
- 3) The GEM regional model predicted cloud coverage and precipitable water [a threshold of  $35 \text{ kg m}^{-2}$  used for operationally forecasting severe rainfall; see Johnson and Moser (1992) and Mainville (2004)] are assessed with the NARR.

The GEM regional model uses a comprehensive physics package (Mailhot et al. 1998), which allows us to simultaneously take into account both convective and stratiform precipitation. For the explicit (grid resolvable) condensation, the scheme developed by Sundqvist (1978) and Sundqvist et al. (1989) is used for stratiform precipitation. The Kain–Fritsch (referred to as KF; see Kain and Fritsch 1990, 1993; Kain et al. 2003; Kain 2004) and the Kuo transient (Ktrans, e.g., Mailhot et al. 2006; Bélair et al. 2005) schemes are used for deep and shallow convection, respectively. Also, the MoisTKE boundary layer cloud scheme (Mailhot et al. 2006; Bélair et al. 2005) is employed. In the explicit scheme (Sundqvist et al. 1989), cloud fraction  $C$  is diagnosed in terms of relative humidity (RH):

$$C = 1 - \sqrt{\frac{1 - \text{RH}}{1 - \text{RH}_{\text{crit}}}}, \quad (1)$$

where  $\text{RH}_{\text{crit}}$  is a critical RH above which cloud is assumed to form. In the deep convection scheme, the cloud fraction is calculated based on updraft mass flux, including detrainment from deep convection [see Kain et al. (2003) and Kain (2004) for details], and in the shallow convection scheme (Mailhot et al. 2006; Bélair et al. 2005), the cloud fraction is computed based on in-cloud values of temperature and specific humidity, as well as the cloud water content [see Eq. (16) of Bélair et al. (2005) for details]. In the MoisTKE boundary layer cloud scheme, the cloud fraction is a nonlinear function of the normalized saturation deficit [see Eq. (6) of Bélair et al. 2005 for details].

The maximum-random overlap assumption is employed to determine cloud coverage in the low, middle,

and high levels; that is, the overlap is a maximum when the cloud layers are connected and random when they are separated by clear sky.

The KF scheme relates the intensity of deep convection to CAPE and triggers convective activity when the vertical motion  $w$  is greater than a threshold  $c(z)$  at the lifting condensation level (LCL). Based on the KF closure assumption, the mass in an atmospheric column is rearranged using the updraft, downdraft, and environmental mass fluxes until at least 90% of CAPE is removed.

- 4) The model-predicted CAPE and soundings are evaluated against the observed CAPE and soundings obtained from the University of Wyoming as well as the NARR.

The NARR dataset has been widely used (e.g., Milrad et al. 2011, 2014; Carrera et al. 2009; Langlois et al. 2009; Bukovsky and Karoly 2007; Becker and Berbery 2009). Ideally, we should routinely use high-resolution observations to verify the GEM regional model predicted fields. Unfortunately, there are no such routine high-resolution observations available. For example, a low pressure system center is usually not located at any given climate station so that a central MSLP of the weather system cannot be verified against the station observations. Our choice is therefore to use the high-resolution NARR data that are independent from the GEM forecasts.

### 3. Severe rainfall in Ottawa on 24 July 2009

#### a. Overview

The Ottawa–24 July SSR event involved three northwest–southeast-orientated extratropical cyclones labeled as A, B, and C at 0300 UTC 24 July 2009 (Fig. 1). Cyclone B, with a central MSLP of 1008 hPa, was closely associated with rainfall development over the Ottawa area, particularly during the early morning of 24 July.

The rain gauge at Ottawa received daily precipitation (added up from hourly rainfall observations) of 67.2 mm on 24 July 2009 (Table 1). Since there is a 4-h difference between eastern daylight time (EDT) and UTC (i.e., EDT = UTC – 4), we examine the GEM regional model accumulated rainfall from 0000 to 2400 EDT (i.e., between 0400 UTC 24 July and 0400 UTC 25 July). Table 1 shows that the model predicts the daily accumulated precipitation to be about 5 mm, which is much less than the rain gauge–observed 67.2 mm and the radar-measured 75–100 mm. Hence, this SSR event was missed by the operational model forecast in terms of rainfall intensity and location. Even with the experimental GEM 2.5-km resolution model forecast, it only produces about 23 mm

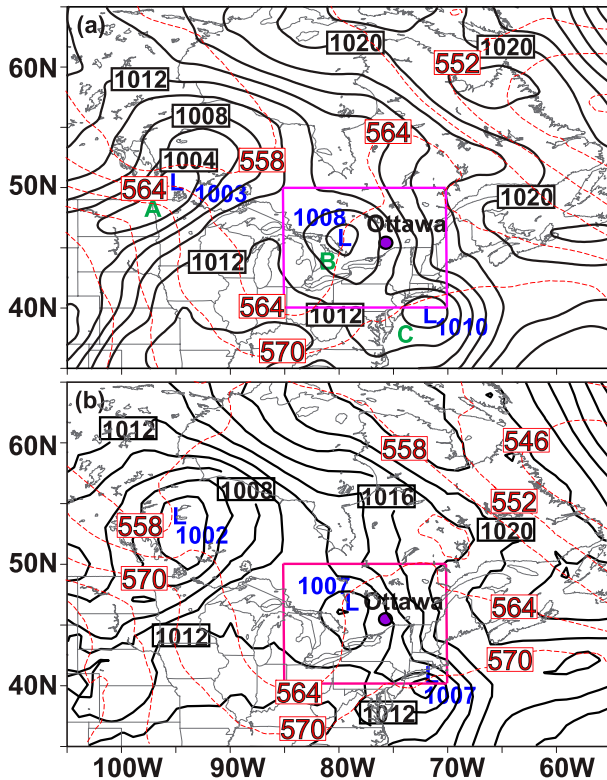


FIG. 1. MSLP (black solid lines) and 500–1000-hPa thickness (red dashed lines) at 0300 UTC 24 Jul 2009 for the (a) NARR and (b) GEM regional model forecasts. The dot indicates the location of Ottawa.

of rainfall in 24 h (not shown). This SSR event was also missed by operational forecasters since there was no watch and/or warning issued for the Ottawa area from the beginning to the end of the SSR event.

While the GEM regional model missed the SSR event, it does not mean that the model-predicted rainfall has no value to forecasters. In fact, during the time period of 0000–0400 UTC 24 July the GEM regional model predicted a rainfall maximum of 31 mm, but it was located a few hundred kilometers away from Ottawa (Fig. 2). The location and timing errors can be traced

back to the model initial conditions, showing that the model initial position of cyclone B is about 400 km to the north-northwest of the NARR estimate (Fig. 3). Although the position error of surface cyclone B decreases with time, its interaction with cyclones A and C (the detailed discussion on cyclone interaction will be presented in a separate paper), as well as its vertical coupling with the upper-level disturbances, could distort the large-scale forcing associated with the SSR generation at the right location and timing.

Because the model-predicted cyclone B moves too fast to the northwest, it departs substantially from the Ottawa area. Thus, the corresponding meteorological variables, such as vertical velocity, cloud, and CAPE, differ from the NARR values.

### b. Lifting mechanism

Figure 4 compares the NARR and the model-predicted omega  $\omega$  field at 700 hPa. The magnitude of the NARR  $\omega$  field over the area of interest varies from  $-1.8$  to  $1.0 \text{ Pa s}^{-1}$  (Fig. 4a) whereas the model prediction changes from  $-4.2$  to  $0.8 \text{ Pa s}^{-1}$  (Fig. 4b). The major difference is that the NARR  $\omega$  field is all negative from the southeast corner of the domain northwestward through the Ottawa area (Fig. 4a), whereas the GEM  $\omega$  has at least three positive bands embedded in this region, including Ottawa (Fig. 4b). Zooming in on the Ottawa area, we find that the NARR  $\omega$  has a value of about  $-0.6 \text{ Pa s}^{-1}$  (Fig. 4a) whereas the model prediction is around  $0.2 \text{ Pa s}^{-1}$  (Fig. 4b). This opposite sign in  $\omega$  between the NARR and the model prediction indicates that the NARR produces upward motion in Ottawa but the model prediction generates downward motion, inhibiting the triggering of the parameterized convection and condensation. On the other hand, to the northwest of Ottawa the GEM produces upward motion, matching up with the model error in the cyclone track.

We have also compared the geopotential height at 0300 UTC between the NARR and the model predictions. As shown in Fig. 5, the NARR-generated

TABLE 1. Comparison of 24-h rainfall accumulation in Ottawa ( $45.42^\circ\text{N}$ ,  $75.70^\circ\text{W}$ ) and its vicinity between observations available on 24 Jul 2009 and the GEM regional model forecast.

Source	Location or station name (ID)	Distance from the measurement point to Ottawa (km) <sup>a</sup>	24-h rainfall accumulation (mm)
Radar	Franktown, ON	—	75–100
Rain gauge	Ottawa CDA RCS (ID 6105978)	4.71	67.2
GEM regional model forecast	—	—	5

<sup>a</sup> Value is calculated based on the distance between the surface station and Parliament Hill in Ottawa.

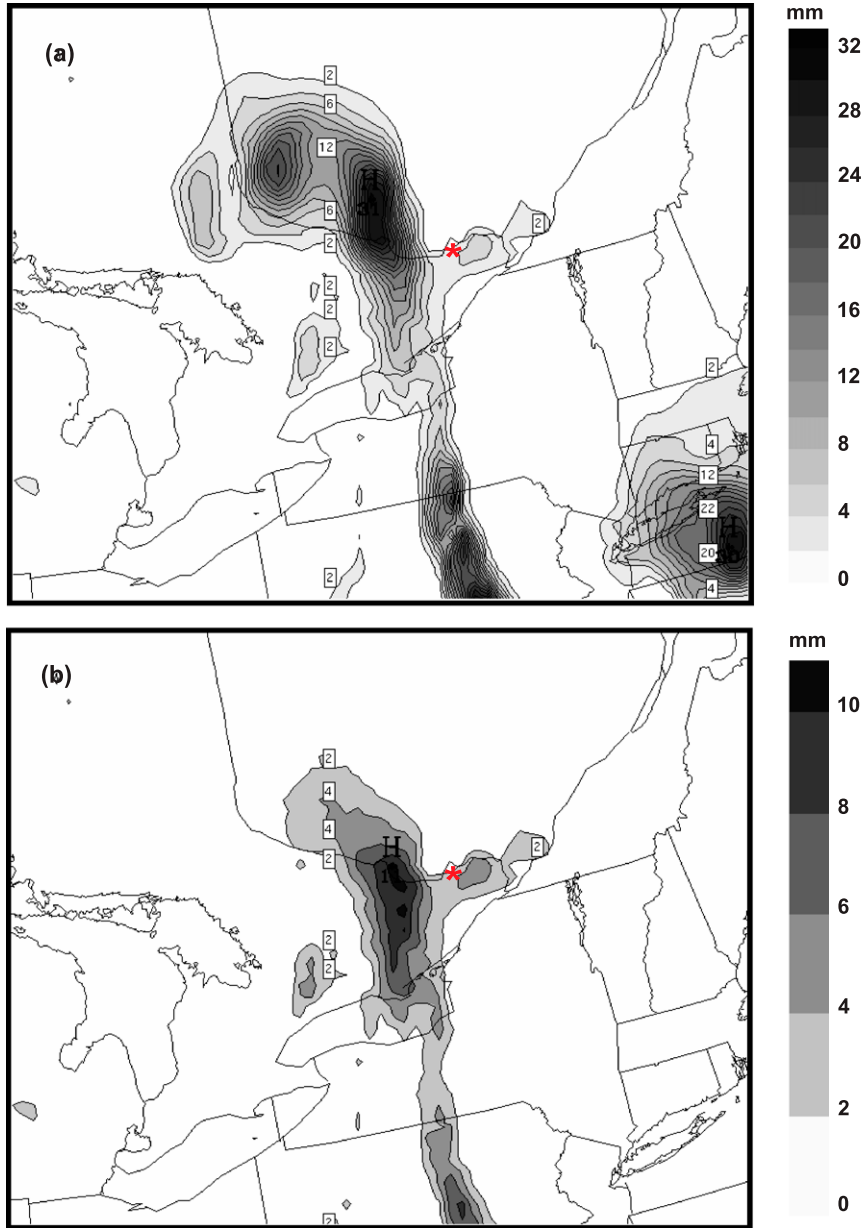


FIG. 2. The GEM regional model predicted precipitation accumulation (mm) from 0000 to 0400 UTC 24 Jul 2009 based on (a) the grid-resolvable scheme and (b) the parameterized convection scheme. The geographic location of Ottawa is indicated by the red star.

closed cyclone B at 1000 hPa corresponds to open troughs at 700 and 500 hPa, indicating that cyclone B in the NARR is westerly tilted with height. This suggests that the differential vorticity advection in the NARR contributes to the upward motion over Ottawa. However, the model-predicted cyclone B is vertically stacked (i.e., the closed lows at 1000-, 700-, and 500-hPa pressure surfaces are located at a similar horizontal position), likely because of the model-predicted cyclone B moving too fast in the northwest direction, indicating little

contribution of differential vorticity advection to the upward motion in the area of interest. Furthermore, the 500-hPa trough in the NARR is considerably more negatively tilted than in the GEM regional model. This indicates stronger differential cyclonic vorticity advection and apparently a more intense surface cyclone downstream. However, both the NARR and the model show little warm-air advection in the Ottawa area at 0300 UTC, as indicated by weak 500–1000-hPa thickness gradients (dashed red lines in Fig. 1).

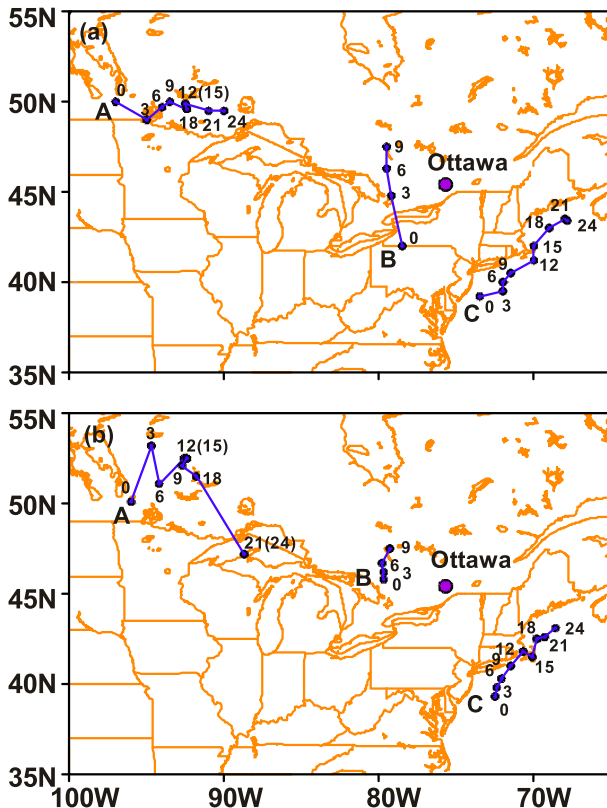


FIG. 3. Tracks of three surface cyclones (A, B, and C) based on the (a) NARR and (b) GEM regional model forecasts at hours (UTC) labeled along the cyclone paths. The dot indicates Ottawa.

The dynamically driven lifting for the SSR development can be also realized through the low-level jet (LLJ) [ $\geq 12 \text{ m s}^{-1}$ ; see Bonner (1968), Whiteman et al. (1997), and Zhang et al. (2006)] development. Comparisons between the NARR vertical motion field and the 850-hPa LLJ indicate that Ottawa is located in the left-exit region of the LLJ and in the area of upward motion at the same time (not shown). The left-exit region of LLJs is conducive to SSR development (e.g., Alliksaar 2007; Kumjian et al. 2006) through providing cyclonic vorticity and low-level moisture convergence. On the other hand, the model-forecasted LLJ left-exit region is away from the Ottawa area where a downward motion is present.

### c. Moisture availability and cloud

Given that the model-predicted rainfall mostly appears during the period of 0000–0400 UTC 24 July, we further examine the moisture availability and atmospheric instability during this time frame. For this event, both the NARR and the model-predicted precipitable water in Ottawa at 0300 UTC are in a range of 37–40  $\text{kg m}^{-2}$ , which is greater than a 35  $\text{kg m}^{-2}$  threshold for forecasting SSR in operation (Johnson and Moser

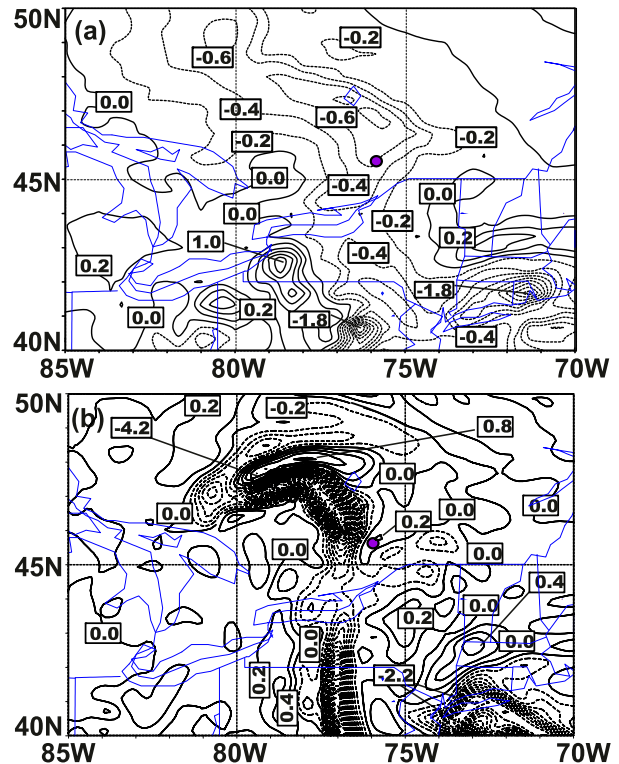


FIG. 4. The 700-hPa  $\omega$  fields with a contour interval of  $0.2 \text{ Pa s}^{-1}$  (dashed lines for negative values of upward motion and solid lines for positive values of downward motion) at 0300 UTC 24 Jul 2009 from the (a) NARR and (b) GEM regional model forecasts. The dot indicates Ottawa.

1992). To determine how efficiently water vapor is converted into cloud water, we compare the cloud coverage between the NARR and the GEM regional model forecast.

Table 2 shows a point (in Ottawa) comparison of cloud coverage between the NARR and model-predicted values. The NARR low-, middle-, and high-level cloud<sup>2</sup> coverages at 0300 UTC in Ottawa are 60%–80%, 60%–80%, and >80%, respectively, whereas the model-predicted coverages are about >85%, 28%, and 44%. At 1500 UTC, these differences become more substantial: for NARR the low-, middle-, and high-level cloud coverage percentages are 60%–80%, >60%, and 80%–100%, respectively, while the model predictions are around 100%, 27%, and 0%, respectively. This indicates that the model forecast has a low efficiency when converting the water vapor into cloud water at the middle and high levels. This also occurs in large areas surrounding the Ottawa region.

<sup>2</sup> High-, middle-, and low-level clouds are defined as the clouds at >6, 2–6, and <2 km, respectively. Additional information may be found online ([http://www.atmos.illinois.edu/earth\\_atmosphere/clouds.html](http://www.atmos.illinois.edu/earth_atmosphere/clouds.html)).

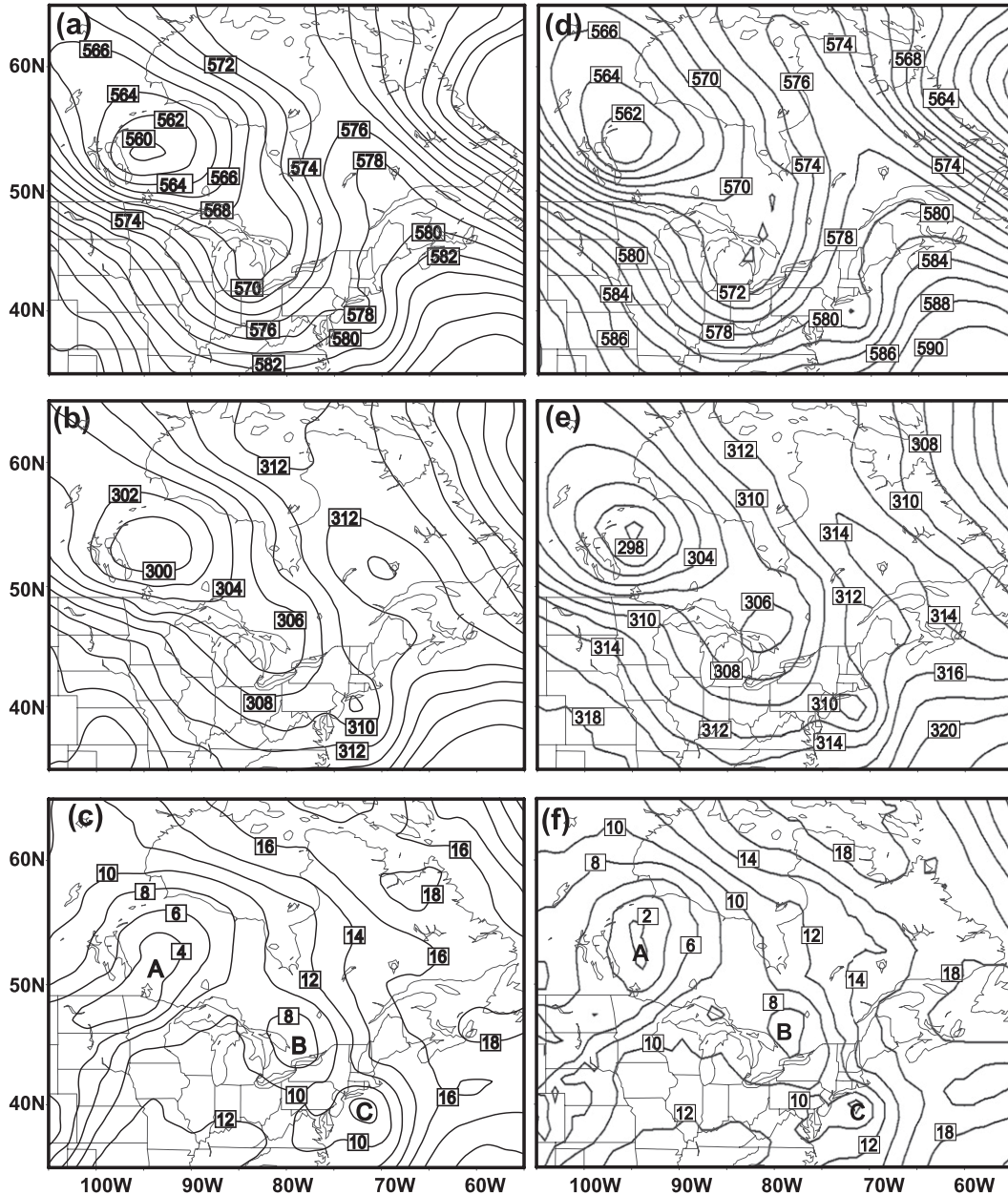


FIG. 5. Geopotential height (in dam) at 0300 UTC 24 Jul 2009 for NARR at (a) 500, (b) 700, and (c) 1000 hPa, and for the GEM regional model at (d) 500, (e) 700, and (f) 1000 hPa.

Figure 6 compares the high- and low-level cloud coverage amounts between the NARR and the GEM regional model forecast. As denoted by an inner box to the south and southeast of Ottawa, the high-level cloud of the NARR varies from 66% to 99% (Fig. 6a) while the model-predicted high-level cloud changes from 33% to 66% (Fig. 6c). The opposite is true for the low levels, for example, the NARR cloud is about 33%–66% (Fig. 6b) but the model-predicted cloud

ranges from 66% to 99% (Fig. 6d). As shown by another inner box to the northwest of Ottawa, at the high level, the NARR cloud coverage in the area of roughly 46°–48°N and 77°–81°W is around 99% (Fig. 6a) whereas the model-predicted coverage is about 33%–66% (Fig. 6c). For the low-level cloud coverage, on the other hand, the NARR estimates about 33%–66% in the same region (Fig. 6b) whereas the model-predicted coverage is about 99% (Fig. 6d).

TABLE 2. Comparison of cloud coverage between the NARR and the GEM regional model forecasts for two cases in Ottawa (45.42°N, 75.70°W) and one in Hamilton (43.25°N, 79.87°W).

Cloud coverage (%)		0300 UTC 24 Jul 2009, Ottawa	1500 UTC 24 Jul 2009, Ottawa	1500 UTC 26 Jul 2009, Hamilton
Low level	NARR	60–80	60–80	60
	GEM regional model	>85	100	90
Middle level	NARR	60–80	>60	50
	GEM regional model	28	27	30
High level	NARR	>80	80–100	80
	GEM regional model	44	0	0

All of these results indicate that the model-predicted maximum latent heating appears at relatively lower levels.

To quantify the model-predicted downward shift of heating maximum, we have calculated condensational heating  $-L(dq_s/dt)$  profiles using the following equation (a detailed derivation can be found in appendix A):

$$-L \frac{dq_s}{dt} = -LF\omega \quad \text{when } \omega < 0, \quad (2)$$

where  $L$  is the latent heat of condensation and  $q_s$  is the saturated specific humidity,  $\omega (=dp/dt)$  is the vertical velocity in  $p$  coordinates, and  $F$  is the so-called condensation function defined by

$$F = \frac{q_s T}{p} \left( \frac{LR - C_p R_w T}{C_p R_w T^2 + q_s L^2} \right), \quad (3)$$

where  $T$  and  $p$  are temperature and pressure;  $R$ ,  $R_w$ , and  $C_p$  are the gas constant, water vapor constant, and specific heat at constant pressure, respectively. Figure 7 compares condensational heating profiles between the NARR and the GEM regional model forecast. At 0300 UTC 24 July, the maximum condensation heating in the NARR is located at 700 hPa, whereas the model-predicted level is positioned at 925 hPa, shifting about 225 hPa downward.

As pointed out by Zhang et al. (1988, 1994), the downward shift of maximum heating is mainly caused by an explicit (grid-resolvable) scheme, which generally

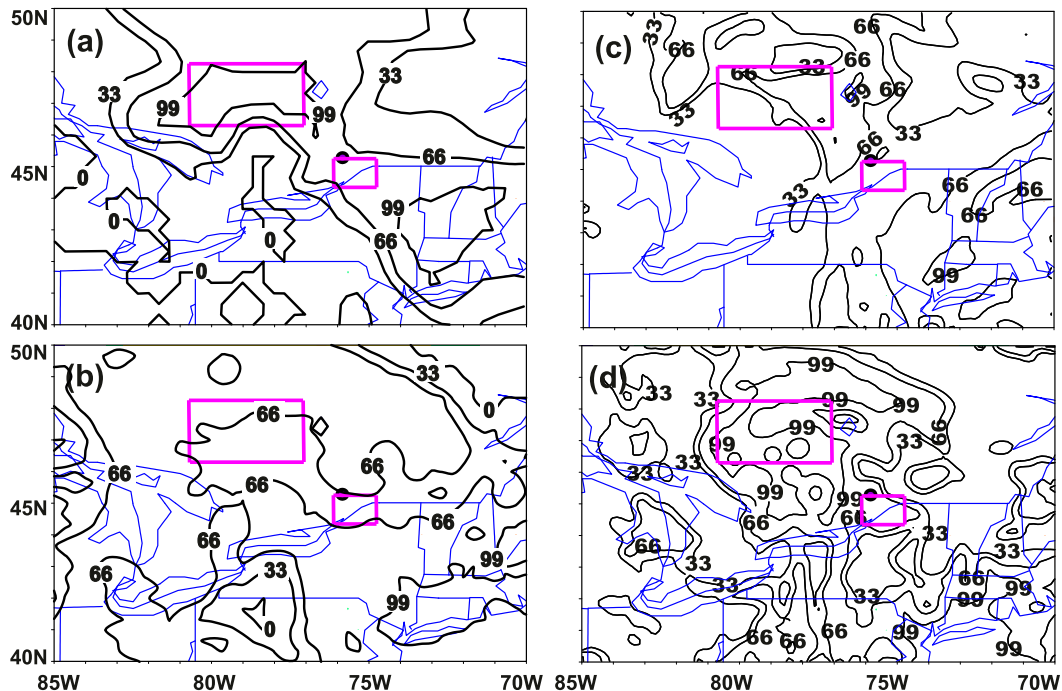


FIG. 6. The NARR cloud coverage (%) at (a) high and (b) low levels, and the GEM regional model predicted cloud coverage (%) at (c) high and (d) low levels at 0300 UTC 24 Jul 2009. The dot indicates Ottawa. Two inner boxes (with a pink color; see text for details) are located to the south and southeast, and to the northwest, of Ottawa, respectively.

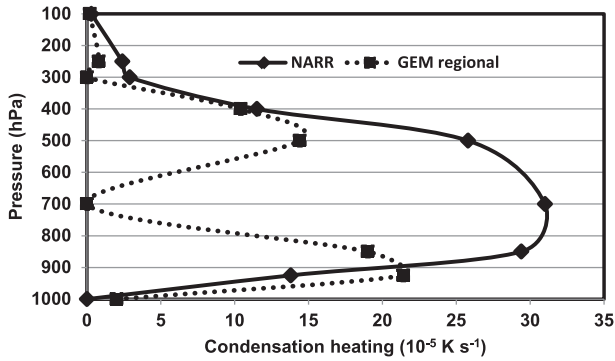


FIG. 7. Condensation heating in Ottawa at 0300 UTC 24 Jul 2009 from the NARR and the GEM regional model forecasts.

exhibits a heating maximum at a relatively lower level than the parameterized convection scheme. In this case, the grid-resolvable precipitation dominates over the parameterized convective precipitation (cf. Figs. 2a,b), which is consistent with the latent heating peaking at the lower levels, as shown in Fig. 7. This dominant grid-scale precipitation may be attributed to insufficient CAPE for the parameterized deep convection, as will be discussed in section 3d. The lack of deep convection, therefore, results in less rainfall in the model for this SSR event.

#### d. Atmospheric instability

As mentioned before, we suspect the presence of smaller CAPE in the model atmosphere because of the model-predicted lower convective precipitation. For this reason, we compare the model CAPE with the NARR CAPE in Table 3 and plot Fig. 8 to compare the model soundings to the NARR soundings in Ottawa. As shown in Table 3, the model-predicted CAPE is only  $148.8 \text{ J kg}^{-1}$  in Ottawa, whereas the NARR CAPE is  $690.5 \text{ J kg}^{-1}$ . Since a maximum vertical velocity of a rising parcel is proportional to CAPE (i.e.,  $w_{\text{max}} = \sqrt{2\text{CAPE}}$ ), the model-predicted low CAPE certainly has impacts on vertical motion as shown in section 3b. On the other hand, both the NARR and the model show little warm advection in the Ottawa area at 0300 UTC, which is implied by the small vertical wind shear (Fig. 8).

At 0300 UTC 24 July the model sounding is cooler ( $\sim 18^\circ\text{C}$ ) at the surface than is the NARR ( $\sim 21^\circ\text{C}$ ). This may be due to more cloud presence during the nighttime in the NARR (especially at the middle and high levels) than is found for the model, although the model cloud is slightly higher at the low level. As a result, more clouds trap more heat emitted from the surface and reemit back toward the surface, leading to a higher surface temperature in the NARR. Another noticeable difference is that the model-predicted temperature profile has a

TABLE 3. Comparison of CAPE ( $\text{J kg}^{-1}$ ) between the NARR and the GEM regional model forecasts for two cases in Ottawa ( $45.42^\circ\text{N}$ ,  $75.70^\circ\text{W}$ ) and one in Hamilton ( $43.25^\circ\text{N}$ ,  $79.87^\circ\text{W}$ ).

	0300 UTC 24 Jul 2009, Ottawa	1500 UTC 26 Jul 2009, Hamilton
NARR	690.5	672.0
GEM regional model	148.8	0.0

much smaller vertical temperature gradient of  $5^\circ\text{C}$  over the lowest 150-hPa model layer than does the NARR value of  $8^\circ\text{C}$  over the lowest 150-hPa layer (Fig. 8). In other words, the model-predicted temperature changes from  $\sim 18^\circ\text{C}$  at 1000 hPa to  $\sim 13^\circ\text{C}$  at 850 hPa and has no temperature change at the lowest 80-hPa model layer whereas the NARR temperature changes from  $\sim 21^\circ\text{C}$  at 1000 hPa to  $\sim 13^\circ\text{C}$  at 850 hPa (Fig. 8). This finding indicates that the model is overmixing in the vertical. The overmixing is likely caused by a stronger LLJ near Ottawa in the model ( $\sim 26 \text{ m s}^{-1}$  at 850 hPa) than is found for the NARR ( $\sim 16 \text{ m s}^{-1}$  at 850 hPa) (not shown). McTaggart-Cowan and Zadra (2015) found that excessive vertical mixing in the planetary boundary layer (PBL) scheme is responsible for the model prediction error in temperature of about  $10^\circ\text{C}$  for a freezing rain event that occurred on 22 March 2007 over the Ontario and Quebec regions, contributing to the late issuance of the freezing rain warnings. By introducing Richardson (Ri) number hysteresis into the PBL scheme, McTaggart-Cowan and Zadra (2015) improved the model-predicted temperature for this case through suppressing the generation of turbulent kinetic energy (TKE) and mixing thereby. Their scheme has a positive impact on this stable winter case, but it shows relatively little impact on summer cases because of the prevalence of an unstable PBL (McTaggart-Cowan and Zadra 2015).

## 4. Severe rainfall around Hamilton on 26 July 2009

### a. Overview

The Hamilton–26 July SSR event was associated with a quasi-stationary low pressure system over central Ontario (Figs. 9a,b). The severe rainfall caused flash flooding on highways and parking lots, and in the basements around the Hamilton area.

The radar at King City, Ontario, observed 50–75-mm rainfall in 24 h around the city of Hamilton (Table 4). However, the model-predicted 24-h accumulated precipitation is between 5 and 10 mm (Table 4). The GEM 2.5-km-resolution model forecasts only about 3 mm of rainfall in 24 h (not shown). A further examination of the radar observations reveals a well-defined linear rainband that propagated across the Hamilton area at 1500 UTC 26 July, while the operational model did not

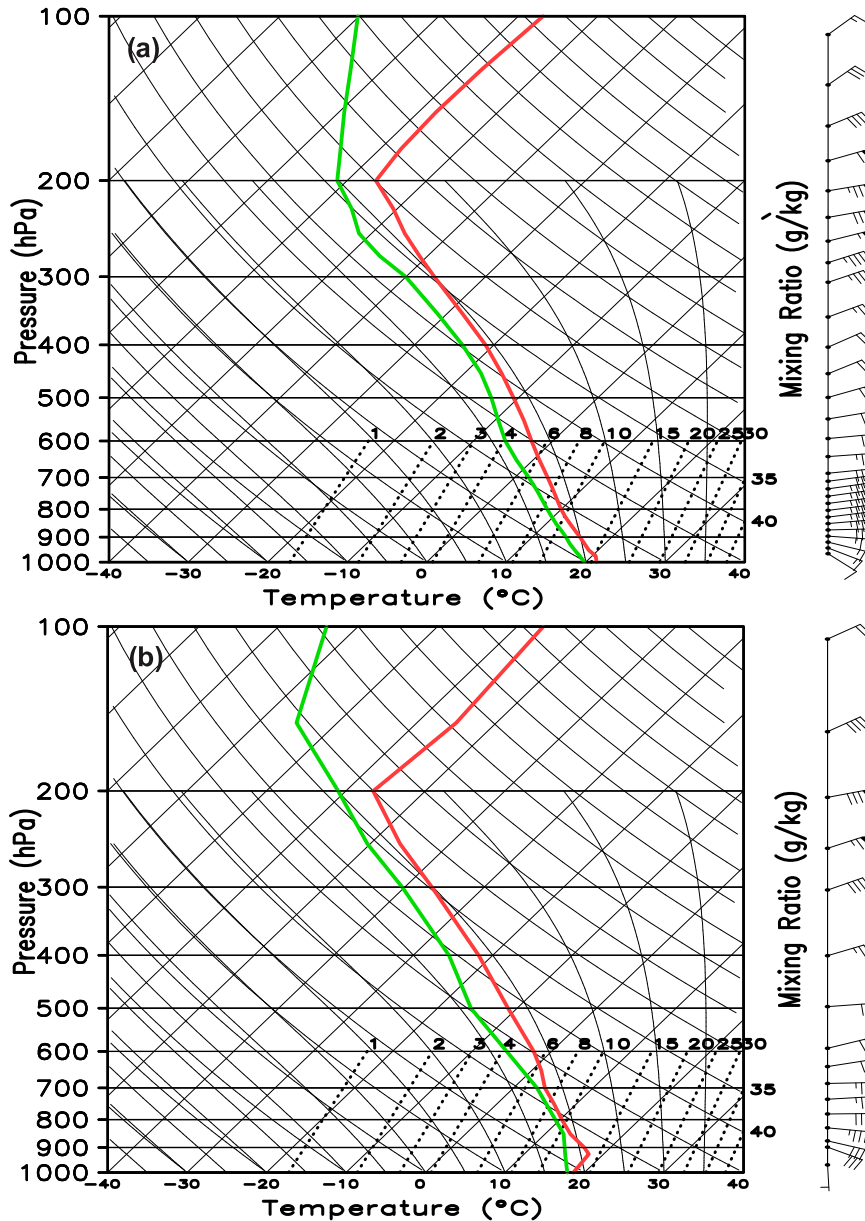


FIG. 8. Atmospheric soundings (red lines represent temperature and green lines stand for dewpoint temperature) at 0300 UTC 24 Jul 2009 for the (a) NARR and (b) GEM regional model forecasts.

forecast the formation of such a linear convective system, so little precipitation was predicted (Fig. 10). In reality, there were repeated formations and movements of such rainband structures across the Hamilton area (e.g., 1600 and 1700 UTC; see Fig. 10), like the echo-training phenomena (Doswell et al. 1996). Similar phenomena had been observed in other SSR studies (e.g., Schumacher and Johnson 2005, 2008, 2009; Zhang and Zhang 2012; Luo et al. 2014). Zhang et al. (2013) showed that reproducing the periodic initiation and subsequent

propagation of convective cells along the same path (i.e., the echo-training process) may require the use of high-resolution cloud-permitting NWP models.

The Hamilton–26 July SSR event was considered to have been missed by operational forecasters because the severe thunderstorm watch and/or warning was issued about 2.5 h after its occurrence (i.e., at 1500 UTC 26 July; see appendix B for details). To understand why the operational model misses this SSR event, it is desirable to examine this event from the viewpoint of lifting mechanism,

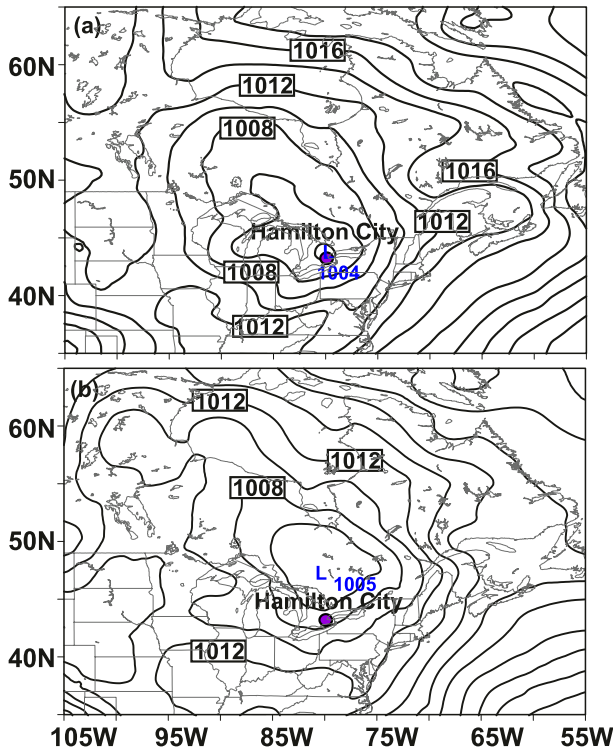


FIG. 9. MSLP (hPa) from the NARR at (a) 0000 UTC 26 Jul and (b) 0000 UTC 27 Jul 2009. The dot indicates Hamilton.

moisture availability, and instability. Since the most intense rainfall occurred around 1500 UTC, we will pay more attention to the meteorological conditions around this time.

### b. Lifting mechanism

The NARR 700-hPa  $\omega$  field is compared to the model-predicted estimate in Fig. 11, showing that over the domain the former  $\omega$  changes from  $-0.6$  to  $0.2 \text{ Pa s}^{-1}$  (Fig. 11a) while the latter varies from  $-2.5$  to  $0.7 \text{ Pa s}^{-1}$  (Fig. 11b). In Hamilton, the NARR exhibits a negative value of about  $-0.1 \text{ Pa s}^{-1}$  for upward motion (Fig. 11a), but the model-predicted estimate has a very small positive value close to zero (Fig. 11b). Consistently, the left-exit region of the NARR-analyzed 700-hPa LLJ is located in the Hamilton area, favorable for moisture transport and the upward motion, whereas the model-predicted left-exit region of the 700-hPa LLJ is misplaced to the northeast of Lake Ontario, conducive to downward motion around the Hamilton area (not shown). This indicates that the model atmosphere in the Hamilton region becomes unfavorable for lifting. Clearly, in order for the echo-training process to be operative, a long period of favorable uplifting should be available, even when a cloud-permitting NWP model is used. These details all explain why little rainfall was predicted in Hamilton.

TABLE 4. Comparison of 24-h rainfall accumulation around the city of Hamilton ( $43.25^\circ\text{N}$ ,  $79.87^\circ\text{W}$ ) between observations available on 26 Jul 2009 and the GEM regional model forecast.

Source	Location	24-h rainfall accumulation (mm)
Radar	King City, ON	50–75
GEM regional model forecast	—	5–10

### c. Moisture availability and cloud

In the Hamilton area, both the NARR and the model-predicted precipitable water are about  $30 \text{ kg m}^{-2}$ , but their cloud fields are quite different. Table 2 shows a point comparison in Hamilton between the NARR and the model-predicted clouds. The NARR low-, middle-, and high-level cloud coverages are 60%, 50%, and 80%, respectively, whereas the model-predicted low-, middle-, and high-level cloud coverages are about 90%, 30%, and almost zero, respectively (Table 2). This indicates that the model has a low efficiency when converting the water vapor into cloud water at the middle and high levels.

Similar comparisons are performed over large areas. As denoted by an inner box including Hamilton, the high-level cloud of the NARR is about at least 66% (Fig. 12a) whereas the model-predicted high-level cloud is almost zero (Fig. 12c). The opposite occurs in the low level: as shown in Fig. 12b, the NARR cloud ranges from 33% to 66% but the model-predicted cloud is from 66% to 99% (Fig. 12d). Based on our computation, the model-predicted maximum condensation heating is shifted downward about 100 hPa (Fig. 13). Another inner box to the north of Hamilton shows that the model-predicted high-level cloud fraction is almost zero (Fig. 12c) whereas the NARR is about 66%–99% (Fig. 12a). In the same region, on the other hand, the model-predicted low-level cloud fraction is about 99% (Fig. 12d), whereas the NARR is about 33%–66% (Fig. 12b). This indicates that the model-predicted maximum latent heating occurs at relatively lower levels. Like the Ottawa–24 July case, the grid-resolvable precipitation dominates the parameterized convective precipitation. As will be discussed in section 4d, this is again attributed to insufficient CAPE for the parameterized deep convection. Less precipitation is generated because of the absence of deep convection activity and the echo-training process.

### d. Atmospheric instability

Table 3 compares the surface-based CAPE between the NARR and the model forecast. At 1500 UTC 26 July, the model-predicted CAPE is  $0.0 \text{ J kg}^{-1}$  in Hamilton whereas the NARR is  $672.0 \text{ J kg}^{-1}$ . A skew  $T$ –log $p$  diagram of the observed sounding at the closest location

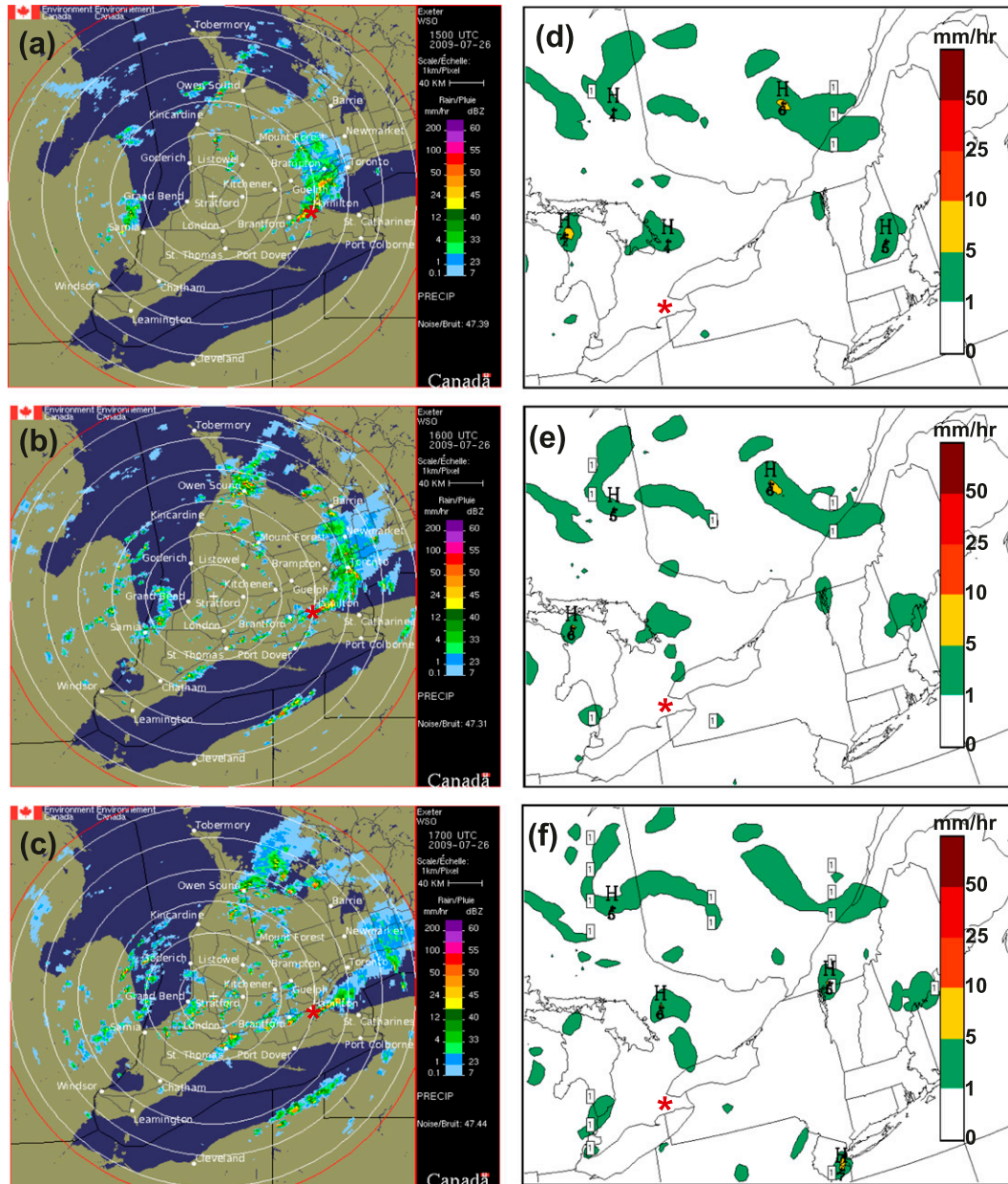


FIG. 10. The radar-observed precipitation rate ( $\text{mm h}^{-1}$ ) at (a) 1500, (b) 1600, and (c) 1700 UTC 26 Jul 2009. (d)–(f) As in (a)–(c), but for the GEM regional model forecast. The geographic location of Hamilton is indicated by a red star.

(Buffalo, New York,  $42.93^{\circ}\text{N}$  and  $78.73^{\circ}\text{W}$ ) at the closest time (1200 UTC) demonstrates a CAPE value of about  $572.8 \text{ J kg}^{-1}$  (not shown). This observed CAPE is similar to the magnitude of the NARR for Hamilton at 1500 UTC 26 July. Therefore, the model predicts little convective instability in the Hamilton area. Because of the model overmixing in the vertical, the model-predicted moisture profile has a smaller vertical specific humidity gradient of  $3.5 \text{ kg kg}^{-1}$  over the lowest 150-hPa model layer than does

NARR, with  $5.0 \text{ kg kg}^{-1}$  over the lowest 150-hPa layer. This overmixing is likely caused by a stronger LLJ near Hamilton in the model ( $\sim 28 \text{ m s}^{-1}$  at 850 hPa) than the NARR ( $\sim 18 \text{ m s}^{-1}$  at 850 hPa) (not shown).

In short, the model-predicted low convective instability and unfavorable large-scale forcing conditions account for little rainfall being produced in the Hamilton area. Even given perfect model initial conditions with realistic CAPE at the time of convective initiation,

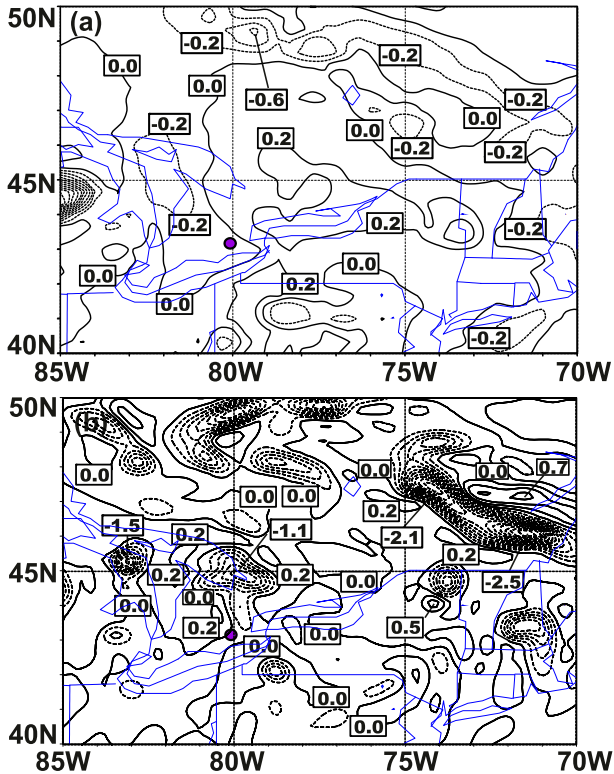


FIG. 11. As in Fig. 4 but for 1500 UTC 26 Jul 2009. The dot indicates Hamilton.

the reproduction of the observed linear rainbands and their subsequent movements along the same path may require the use of a cloud-permitting model to simulate this echo-training process. Schumacher and Johnson (2008) employed convection-permitting simulations to successfully reproduce the quasi-stationary organization and evolution of a mesoscale convective system, but not the exact rainfall amount, associated with destructive flash flooding in eastern Missouri on 6–7 May 2000.

## 5. Concluding remarks

In this study, two missed SSR events that occurred in Ontario, Canada, are examined using the hourly operational 15-km GEM model forecasts, the 3-hourly 32-km resolution NARR data, and the daily rain gauge and radar data, as well as other available observations.

Listed below are some common features from the analyses of the Ottawa–24 July 2009 and Hamilton–26 July 2009 SSR events.

- Over the areas of interest, the NARR  $\omega$  shows upward motion, whereas the model prediction mainly exhibits downward motion that inhibits triggering of the parameterized convection scheme and condensation. This

difference is attributed mainly to the differential vorticity advection mechanism being operated in the NARR but not in the model over the area of interest, and partly to the left-exit region of the NARR-analyzed LLJ being located in the area of interest but not for the model prediction.

- The vertical shifting of the heating maximum to lower levels frequently occurs when the grid-resolvable-scale precipitation dominates the parameterized convection. Under this circumstance, 1) most of moisture at lower levels is consumed through explicit (grid resolvable) condensation processes; 2) for a given amount of moisture available, the parameterized deep convection scheme loses a competition to the explicit scheme; and 3) the lack of triggering deep convection (i.e., low vertical velocity or CAPE) makes the parameterized deep convection scheme unable to transport enough moisture upward for condensation at higher levels. As a result, the lack of deep convection leads to less precipitation for SSR events.
- In addition, the GEM regional model tends to underpredict the conversion of water vapor into cloud water, especially at the middle and high levels, although the model well forecasts the precipitable water.

For the Ottawa–24 July SSR event, the differential vorticity advection, together with the LLJ, plays an important role in rainfall development through providing lifting conditions in a moist environment over Ottawa.

This event primarily involved prediction errors in location, which are likely associated with errors in the model initial conditions. The model-predicted rainfall period appears about 4 h earlier than does the major observed rainfall period. Within this 4-h period, the model-predicted rainfall is horizontally shifted to an inaccurate location, which can be attributed to the model-predicted cyclone B moving too far to the northwest of Ottawa, leading to the horizontal shift of vertical motion fields and rainfall as well.

Continuously improving the model initial conditions is very helpful in the accurate prediction of SSR events. To do that, one needs to take more observational data into consideration during the data assimilation processes, including the data obtained from both meteorological organizations (e.g., radar wind and reflectivity data) and nonmeteorological organizations (e.g., data from airplanes and from conservation authorities). For example, the radar wind data, together with other data, will be useful in determining atmospheric circulations, convergence patterns, positions of low (high) pressure systems, and locations of upward (downward) motion.

As mentioned earlier, one of the important parameters for triggering the KF deep convection scheme is the threshold grid-scale vertical velocity  $W_c$ . To trigger the

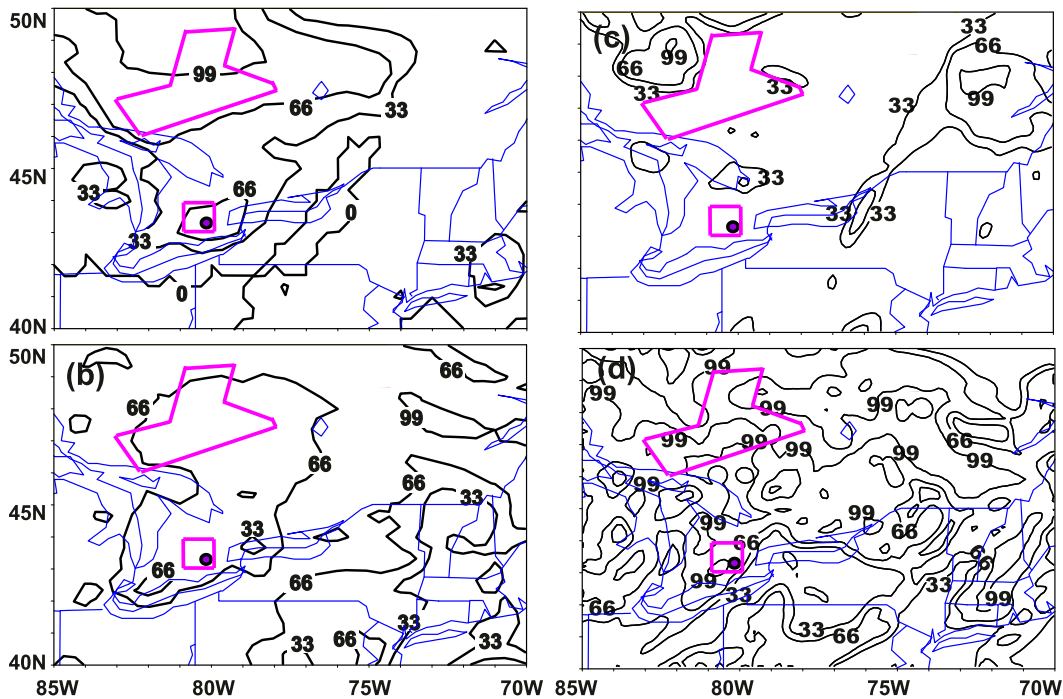


FIG. 12. As in Fig. 6, but at 1500 UTC 26 Jul 2009. The dot indicates Hamilton.

KF scheme at the right locations and times, we need the right sign and magnitude of  $W_i$ . Producing more accurate initial conditions through incorporating more observational data may be helpful in avoiding the model-predicted vertical velocity having an opposite sign to the observed in the area of interest (e.g., the Ottawa–24 July SSR event).

Furthermore,  $W_i$  is dependent upon model resolution, and it needs to be tuned as a function of resolution. Currently, in the GEM regional model  $W_i$  is tuned based on the model horizontal resolution only. It is suggested that  $W_i$  needs to be tuned based on not only the model horizontal but also the model vertical resolution, provided that when the model horizontal resolution increases, the vertical resolution should be increased accordingly. Otherwise, nonphysical noise will be generated because of inconsistencies between the model horizontal and vertical resolutions (e.g., Lindzen and Fox-Rabinovitz 1989; Zhang et al. 2015).

To initiate and maintain convection, CAPE is needed for a parcel to continue rising vertically after its initial displacement. As shown in section 3d, the model sounding is cooler at the surface because of less cloud presence during the nighttime. More importantly, the model-predicted temperature profile has a much smaller vertical temperature gradient over the lowest 150-hPa model layer as a result of overmixing in the PBL, which contributes to low CAPE in the model. Recently, McTaggart-Cowan and Zadra (2015) introduced the

Richardson (Ri) number hysteresis into the PBL scheme to improve the model-predicted temperature for the freezing rain event on 22 March 2007 over the Ontario and Quebec regions through suppressing the generation of TKE and mixing. Their scheme is mainly effective for some winter cases because of the stable PBL assumption. For summer SSR events involved with unstable PBL, based on our knowledge, so far there is no successful scheme for operational NWP models (including the GEM model). This can be an area of further exploration. One possibility is to use a variational method (e.g., Xu and Qiu 1997; Cao and Ma 2005; Cao et al. 2006; Cao and Ma 2009a) to retrieve temperature and moisture profiles in the PBL when sensible and latent heat flux observations are available.

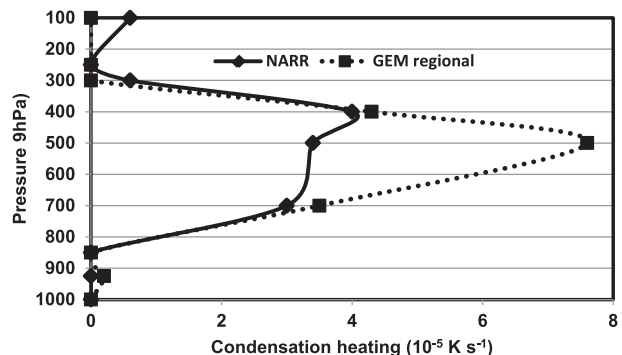


FIG. 13. As in Fig. 7, but for Hamilton at 1500 UTC 26 Jul 2009.

The principle of this variational approach is to minimize the differences between the computed and the observed fluxes so that it can adjust the computed profiles toward the “true” value.

The Hamilton–26 July SSR event was associated with the quasi-stationary low pressure system and the LLJ conducive to the rainfall development, with the most intense rainfall being generated through the echo-training process in a modest CAPE environment.

The echo-training process may require the use of high-resolution cloud-permitting NWP models to simulate the periodic initiation and subsequent propagation of convective cells along the same path, which is difficult for most of the operational NWP models. For example, [Lavers and Villarini \(2013\)](#) recently examined the ability of the world’s most advanced weather forecasting models to predict the 9–16 September 2013 extreme rainfall that caused severe flooding in Boulder, Colorado. They found that these models tended to underestimate rainfall amounts and placed the rainfall in the wrong area, even though they provided an indication that a period of heavy rainfall was going to affect parts of Colorado.

On the other hand, information on the NWP errors in precipitation forecasts may be used to minimize NWP model bias. Also, detailed observational analysis and diagnosis may help improve the prediction of SSR development. Although high-resolution cloud-resolving NWP models may be helpful in predicting SSR events, the proper physical packages (especially when dealing with condensation and precipitation processes) matched with high-resolution NWP models are much more important than increasing model resolutions alone. Since precipitation is an end product of multiscale interactions, there will be always uncertainties in deterministic forecasts although some incremental improvements have been made recently in severe precipitation forecast accuracy (e.g., [Sukovich et al. 2014](#)). As an alternative, ensemble-based NWP predictions might provide some uncertainties for SSR forecasts (e.g., [Buizza et al. 2005](#); [Demeritt et al. 2010](#)), especially the National Center for Atmospheric Research 3-km Ensemble Forecasting System (<http://www.image.ucar.edu/wrfdart/ensemble/index.php>) and the Storm Prediction Center’s Storm-Scale Ensemble of Opportunity (<http://www.spc.noaa.gov/expert/sseo/>).

With the above-mentioned improvements, we hope that the number of missed SSR events will be reduced in the future although some missed SSR events may still inevitably occur.

*Acknowledgments.* We thank Glenn Robinson, a senior forecaster at the Ontario Storm Prediction Center of Environment and Climate Change Canada, for his inputs in identifying missed SSR events over Ontario of Canada;

Dave Patrick for his practical and useful help in solving various problems associated with the scripts and codes for running the radar URP programs; Mark Alliksaar and Helen Yang for their efforts to run the URP programs to generate the radar-observed precipitation accumulation; Victor Chung and Rob Kuhn for carefully reading part of the early version of the manuscript and providing constructive suggestions; and William Burrows and Norman Donaldson for their constructive comments on part of the early version manuscript. We appreciate Dr. Lin Zhu’s assistance with plotting [Figs. 1a, 3, 8, and 9](#). We also appreciate the anonymous reviewers for their suggestions and comments to improve the quality of this paper. The operational GEM regional model forecast data are obtained from the Canadian Meteorological Centre. NCEP–NCAR reanalysis data are provided by the NOAA/OAR/ESRL/PSD, Boulder, Colorado, from their Web site (<http://www.esrl.noaa.gov/psd/>). The observed surface precipitation data and part of the radar images are obtained from the Data Analysis and Archive Division of Environment and Climate Change Canada. The atmospheric soundings are obtained from University of Wyoming. DLZ was supported by ONR Grant N000141410143 and NASA Grant NNX12AJ78G.

## APPENDIX A

### Derivation of Condensation Heating Eq. (2)

Condensational heating  $-L(dq_s/dt)$  can be derived from the Clausius–Clapeyron equation and the first law of thermodynamics. Based on the definition of saturated specific humidity,  $q_s = 0.622(E/p)$ , where  $E$  is saturated water vapor, we have

$$\frac{1}{q_s} \frac{dq_s}{dt} = \frac{1}{E} \frac{dE}{dt} - \frac{\omega}{p}, \quad (\text{A1})$$

where  $\omega (=dp/dt)$  is the vertical velocity in a pressure coordinate. Substituting the Clausius–Clapeyron equation,

$$\frac{1}{E} \frac{dE}{dt} = \frac{L}{R_w T^2} \frac{dT}{dt}, \quad (\text{A2})$$

into (A1), yields

$$\frac{1}{q_s} \frac{dq_s}{dt} = \frac{L}{R_w T^2} \frac{dT}{dt} - \frac{\omega}{p}. \quad (\text{A3})$$

Considering a moist-adiabatic process involved in condensation heating  $-L(dq_s/dt)$  only, we can write the first law of thermodynamics as follows:

$$-L \frac{dq_s}{dt} = C_p \frac{dT}{dt} - \frac{RT}{p} \omega. \quad (\text{A4})$$

Eliminating  $dT/dt$  from Eqs. (A3) and (A4), we obtain

$$-L \frac{dq_s}{dt} = -L \frac{q_s T}{p} \left( \frac{LR - C_p R_w T}{C_p R_w T^2 + q_s L^2} \right) \omega \quad \text{when} \quad \omega < 0. \quad (\text{A5})$$

## APPENDIX B

### Watches/Warnings Issued by the OSPC for Hamilton at 1326 EDT 26 July 2009

WVCN11 CWTO 261726  
SEVERE WEATHER BULLETIN  
ISSUED BY ENVIRONMENT CANADA  
AT 1:26 p.m. EDT SUNDAY 26 JULY 2009.

-----  
WATCHES/WARNINGS IN EFFECT FOR SOUTHERN ONTARIO...

SEVERE THUNDERSTORM WARNING FOR:  
=NEW= CITY OF HAMILTON.

...VERY HEAVY RAIN CONTINUES TO AFFECT THE HAMILTON AREA...

THIS IS A WARNING THAT SEVERE THUNDERSTORMS ARE IMMINENT OR OCCURRING IN THESE REGIONS. REMEMBER SOME SEVERE THUNDERSTORMS PRODUCE TORNADOES...LISTEN FOR UPDATED WARNINGS. EMERGENCY MANAGEMENT ONTARIO RECOMMENDS TAKING COVER IMMEDIATELY WHEN THREATENING WEATHER APPROACHES.

-----  
==DISCUSSION==

RADAR IS DETECTING NEARLY STATIONARY THUNDERSTORMS AFFECTING THE HAMILTON AREA WITH VERY HEAVY RAIN. BASED ON RADAR IT IS POSSIBLE THAT AS MUCH AS 50 TO 75 MILLIMETRES OF RAIN MAY HAVE ALREADY OCCURRED WITH FURTHER AMOUNTS OF 25 TO 50 MILLIMETRES POSSIBLE DURING THE NEXT FEW HOURS.

PLEASE REFER TO THE LATEST PUBLIC FORECASTS FOR FURTHER DETAILS.

END/OSPC

-----  
WVCN11 CWTO 261859  
SEVERE WEATHER BULLETIN  
ISSUED BY ENVIRONMENT CANADA  
AT 2:59 p.m. EDT SUNDAY 26 JULY 2009.

-----  
WATCHES/WARNINGS ENDED FOR SOUTHERN ONTARIO...

SEVERE THUNDERSTORM WARNING ENDED FOR:  
CITY OF HAMILTON.

THE THUNDERSTORMS WHICH PRODUCED LOCALLY VERY HEAVY RAIN IN THE HAMILTON AREA HAVE NOW WEAKENED AND BECOME ISOLATED.

-----  
==DISCUSSION==

PLEASE REFER TO THE LATEST PUBLIC FORECASTS FOR FURTHER DETAILS.

END/..

## REFERENCES

- Alliksaar, M., 2007: Heavy rain event for north-of-Superior – Oct 23, 2004. COMET, UCAR Community Programs, Boulder, CO. [Available online at [http://www.meted.ucar.edu/norlat/cases/detail.php?case\\_number=55&author01=Alliksaar,%20Mark%20&author02=](http://www.meted.ucar.edu/norlat/cases/detail.php?case_number=55&author01=Alliksaar,%20Mark%20&author02=).]
- Appelquist, S., G. E. Gahr, R. L. Pfeffer, and X.-F. Niu, 2002: Comparison of methodologies for probabilistic quantitative precipitation forecasting. *Wea. Forecasting*, **17**, 783–799, doi:10.1175/1520-0434(2002)017<0783:COMFPQ>2.0.CO;2.
- Becker, E. J., and E. H. Berbery, 2009: Understanding the characteristics of daily precipitation over the United States using the North American Regional Reanalysis. *J. Climate*, **22**, 6268–6286, doi:10.1175/2009JCLI2838.1.
- Bélair, S., J. Mailhot, C. Girard, and P. Vaillancourt, 2005: Boundary layer and shallow cumulus clouds in a medium-range forecast of a large-scale weather system. *Mon. Wea. Rev.*, **133**, 1938–1960, doi:10.1175/MWR2958.1.
- Bennett, L. J., K. A. Browning, A. M. Blyth, D. J. Parker, and P. A. Clark, 2006: A review of the initiation of precipitating convection in the United Kingdom. *Quart. J. Roy. Meteor. Soc.*, **132**, 1001–1020, doi:10.1256/qj.05.54.
- Bonner, W. D., 1968: Climatology of the low level jet. *Mon. Wea. Rev.*, **96**, 833–850, doi:10.1175/1520-0493(1968)096<0833:COTLLJ>2.0.CO;2.
- Browning, K. A., 1986: Conceptual models of precipitation systems. *Wea. Forecasting*, **1**, 23–41, doi:10.1175/1520-0434(1986)001<0023:CMOPS>2.0.CO;2.
- , and Coauthors, 2007: The Convective Storm Initiation Project. *Bull. Amer. Meteor. Soc.*, **88**, 1939–1955, doi:10.1175/BAMS-88-12-1939.
- Buizza, R., P. L. Houtekamer, G. Pellerin, Z. Toth, Y. Zhu, and M. Wei, 2005: A comparison of the ECMWF, MSC, and NCEP global ensemble prediction systems. *Mon. Wea. Rev.*, **133**, 1076–1097, doi:10.1175/MWR2905.1.
- Bukovsky, M. S., and D. J. Karoly, 2007: A brief evaluation of precipitation from the North American Regional Reanalysis. *J. Hydrometeorol.*, **8**, 837–846, doi:10.1175/JHM595.1.
- Canadian National Radar Network, 2014: Data analysis and archive division. Environment Canada, accessed 4 February 2016. [Available online at [http://nadm.ontario.int.ec.gc.ca/Intranet/climate/radar\\_extractor/login.cfm](http://nadm.ontario.int.ec.gc.ca/Intranet/climate/radar_extractor/login.cfm).]
- Cao, Z., 2008: Severe hail frequency over Ontario, Canada: Recent trend and variability. *Geophys. Res. Lett.*, **35**, L14803, doi:10.1029/2008GL034888.
- , and J. Ma, 2005: An application of the variational method to computation of sensible heat flux over a deciduous

- forest. *J. Appl. Meteor.*, **44**, 144–152, doi:[10.1175/JAM-2179.1](https://doi.org/10.1175/JAM-2179.1).
- , and —, 2009a: A variational method for computation of sensible heat flux over the Arctic sea ice. *J. Atmos. Oceanic Technol.*, **26**, 838–845, doi:[10.1175/2008JTECHA1214.1](https://doi.org/10.1175/2008JTECHA1214.1).
- , and —, 2009b: Summer severe rainfall frequency trend and variability over Ontario, Canada. *J. Appl. Meteor. Climatol.*, **48**, 1955–1960, doi:[10.1175/2009JAMC2055.1](https://doi.org/10.1175/2009JAMC2055.1).
- , P. Pellerin, and H. Ritchie, 2004: Verification of mesoscale modeling for the severe rainfall event over southern Ontario in May 2000. *Geophys. Res. Lett.*, **31**, L23108, doi:[10.1029/2004GL020547](https://doi.org/10.1029/2004GL020547).
- , J. Ma, and W. R. Rouse, 2006: Improving computation of sensible heat flux over a water surface using the variational method. *J. Hydrometeorol.*, **7**, 678–686, doi:[10.1175/JHM513.1](https://doi.org/10.1175/JHM513.1).
- Carrera, M. L., J. R. Gyakum, and C. A. Lin, 2009: Observational study of wind channeling within the St. Lawrence River valley. *J. Appl. Meteor. Climatol.*, **48**, 2341–2361, doi:[10.1175/2009JAMC2061.1](https://doi.org/10.1175/2009JAMC2061.1).
- Corfidi, S. F., 2003: Cold pools and MCS propagation: Forecasting the motion of downwind-developing MCSs. *Weather Forecasting*, **18**, 997–1017, doi:[10.1175/1520-0434\(2003\)018<0997:CPAMPF>2.0.CO;2](https://doi.org/10.1175/1520-0434(2003)018<0997:CPAMPF>2.0.CO;2).
- , J. H. Meritt, and J. M. Fritsch, 1996: Predicting the movement of mesoscale convective complexes. *Weather Forecasting*, **11**, 41–46, doi:[10.1175/1520-0434\(1996\)011<0041:PTMOMC>2.0.CO;2](https://doi.org/10.1175/1520-0434(1996)011<0041:PTMOMC>2.0.CO;2).
- Côté, J., S. Gravel, A. Méthot, A. Patoine, M. Roch, and A. Staniforth, 1998: The operational CMC/MRB Global Environmental Multiscale (GEM) model. Part I: Design considerations and formulation. *Mon. Wea. Rev.*, **126**, 1373–1395, doi:[10.1175/1520-0493\(1998\)126<1373:TOCMGE>2.0.CO;2](https://doi.org/10.1175/1520-0493(1998)126<1373:TOCMGE>2.0.CO;2).
- Demeritt, D., S. Nobert, H. Cloke, and F. Pappenberger, 2010: Challenges in communicating and using ensembles in operational flood forecasting. *Meteor. Appl.*, **17**, 209–222, doi:[10.1002/met.194](https://doi.org/10.1002/met.194).
- Doswell, C. A., III, H. E. Brooks, and R. A. Maddox, 1996: Flash flood forecasting: An ingredients-based methodology. *Weather Forecasting*, **11**, 560–581, doi:[10.1175/1520-0434\(1996\)011<0560:FFFAIB>2.0.CO;2](https://doi.org/10.1175/1520-0434(1996)011<0560:FFFAIB>2.0.CO;2).
- Fritsch, J. M., and K. F. Heideman, 1989: Some characteristics of the limited-area fine-mesh (LFM) model quantitative precipitation forecasts (QPF) during the 1982 and 1983 warm seasons. *Weather Forecasting*, **4**, 173–185, doi:[10.1175/1520-0434\(1989\)004<0173:SCOTLA>2.0.CO;2](https://doi.org/10.1175/1520-0434(1989)004<0173:SCOTLA>2.0.CO;2).
- , and R. E. Carbone, 2004: Improving quantitative precipitation forecasts in the warm season: A USWRP research and development strategy. *Bull. Amer. Meteor. Soc.*, **85**, 955–965, doi:[10.1175/BAMS-85-7-955](https://doi.org/10.1175/BAMS-85-7-955).
- Gallus, W. A., Jr., N. A. Snook, and E. V. Johnson, 2008: Spring and summer severe weather reports over the Midwest as a function of convective mode: A preliminary study. *Weather Forecasting*, **23**, 101–113, doi:[10.1175/2007WAF2006120.1](https://doi.org/10.1175/2007WAF2006120.1).
- Germann, U., and I. Zawadzki, 2002: Scale-dependence of the predictability of precipitation from continental radar images. Part I: Description of the methodology. *Mon. Wea. Rev.*, **130**, 2859–2873, doi:[10.1175/1520-0493\(2002\)130<2859:SDOTPO>2.0.CO;2](https://doi.org/10.1175/1520-0493(2002)130<2859:SDOTPO>2.0.CO;2).
- Gordon, J. D., and D. Albert, 2012: A comprehensive severe weather forecast checklist and reference guide. National Weather Service, 46 pp. [Available online at [http://www.weather.gov/media/sgf/research/severe\\_weather\\_checklist.pdf](http://www.weather.gov/media/sgf/research/severe_weather_checklist.pdf).]
- Gravelle, C. M., C. E. Graves, J. P. Gagan, F. H. Glass, and M. Evans, 2009: Winter weather guidance from regional historical analogs. Preprints, *23rd Conf. on Weather Analysis and Forecasting/19th Conf. on Numerical Weather Prediction*, Omaha, NE, Amer. Meteor. Soc., JP3.10. [Available online at <https://ams.confex.com/ams/pdfpapers/154201.pdf>.]
- Jessup, S. M., and S. J. Colucci, 2012: Organization of flash-flood-producing precipitation in the northeast United States. *Weather Forecasting*, **27**, 345–361, doi:[10.1175/WAF-D-11-00026.1](https://doi.org/10.1175/WAF-D-11-00026.1).
- Johnson, G. A., and J. Moser, 1992: A decision tree for forecasting heavy rain from mid-latitude synoptic patterns in Louisiana generally from late fall through spring. Post-preprints, *National Heavy Precipitation Workshop*, Pittsburgh, PA, NOAA Tech. Memo. NWS ER-87, 189–194. [Available online at [http://docs.lib.noaa.gov/noaa\\_documents/NWS/NWS\\_ER/TM\\_NWS\\_ER\\_87.pdf](http://docs.lib.noaa.gov/noaa_documents/NWS/NWS_ER/TM_NWS_ER_87.pdf).]
- Kain, J. S., 2004: The Kain–Fritsch convective parameterization: An update. *J. Appl. Meteor. Climatol.*, **43**, 170–181, doi:[10.1175/1520-0450\(2004\)043<0170:TKCPAU>2.0.CO;2](https://doi.org/10.1175/1520-0450(2004)043<0170:TKCPAU>2.0.CO;2).
- , and J. M. Fritsch, 1990: A one-dimensional entraining/detraining plume model and its application in convective parameterization. *J. Atmos. Sci.*, **47**, 2784–2802, doi:[10.1175/1520-0469\(1990\)047<2784:AODEPM>2.0.CO;2](https://doi.org/10.1175/1520-0469(1990)047<2784:AODEPM>2.0.CO;2).
- , and —, 1993: Convective parameterization for mesoscale models: The Kain–Fritsch scheme. *The Representation of Cumulus Convection in Numerical Models, Meteor. Monogr.*, No. 46, Amer. Meteor. Soc., 165–170.
- , M. E. Baldwin, and S. J. Weiss, 2003: Parameterized updraft mass flux as a predictor of convective intensity. *Weather Forecasting*, **18**, 106–116, doi:[10.1175/1520-0434\(2003\)018<0106:PUMFAA>2.0.CO;2](https://doi.org/10.1175/1520-0434(2003)018<0106:PUMFAA>2.0.CO;2).
- Kumjian, M., J. S. Evans, and J. L. Guyer, 2006: The relationship of the Great Plains low level jet to nocturnal MCS development. Preprints, *23rd Conf. on Severe Local Storms*, St. Louis, MO, Amer. Meteor. Soc., P1.11. [Available online at <https://ams.confex.com/ams/pdfpapers/115338.pdf>.]
- Langlois, A., and Coauthors, 2009: Simulation of snow water equivalent (SWE) using thermodynamic snow models in Quebec, Canada. *J. Hydrometeorol.*, **10**, 1447–1463, doi:[10.1175/2009JHM1154.1](https://doi.org/10.1175/2009JHM1154.1).
- Lavers, D. A., and G. Villarini, 2013: Were global numerical weather prediction systems capable of forecasting the extreme Colorado rainfall of 9–16 September 2013? *Geophys. Res. Lett.*, **40**, 6405–6410, doi:[10.1002/2013GL058282](https://doi.org/10.1002/2013GL058282).
- Lindzen, R. S., and M. Fox-Rabinovitz, 1989: Consistent vertical and horizontal resolution. *Mon. Wea. Rev.*, **117**, 2575–2583, doi:[10.1175/1520-0493\(1989\)117<2575:CVAHR>2.0.CO;2](https://doi.org/10.1175/1520-0493(1989)117<2575:CVAHR>2.0.CO;2).
- Lombardo, K. A., and B. A. Colle, 2010: The spatial and temporal distribution of organized convective structures over the northeast and their ambient conditions. *Mon. Wea. Rev.*, **138**, 4456–4474, doi:[10.1175/2010MWR3463.1](https://doi.org/10.1175/2010MWR3463.1).
- Lopez, P., 2007: Cloud and precipitation parameterization in modeling and variational data assimilation: A review. *J. Atmos. Sci.*, **64**, 3766–3784, doi:[10.1175/2006JAS2030.1](https://doi.org/10.1175/2006JAS2030.1).
- Luo, Y., Y. Gong, and D.-L. Zhang, 2014: Initiation and organizational modes in an extreme-rain-producing convective system along a mei-yu front in east China. *Mon. Wea. Rev.*, **142**, 203–221, doi:[10.1175/MWR-D-13-00111.1](https://doi.org/10.1175/MWR-D-13-00111.1).
- Maddox, R. A., 1980: Mesoscale convective complexes. *Bull. Amer. Meteor. Soc.*, **61**, 1374–1387, doi:[10.1175/1520-0477\(1980\)061<1374:MCC>2.0.CO;2](https://doi.org/10.1175/1520-0477(1980)061<1374:MCC>2.0.CO;2).
- , C. F. Chappell, and L. R. Hoxit, 1979: Synoptic and meso- $\alpha$  scale aspects of flash flood events. *Bull. Amer. Meteor. Soc.*, **60**, 115–123, doi:[10.1175/1520-0477-60.2.115](https://doi.org/10.1175/1520-0477-60.2.115).
- Mailhot, J., and Coauthors, 1998: Scientific description of RPN physics library – Version 3.6. Recherche en prévision numérique,

- 188 pp. [Available from RPN, 2121 Trans-Canada, Dorval, QC H9P 1J3, Canada; also online at <http://citeseerx.ist.psu.edu/viewdoc/download?doi=10.1.1.453.7227&rep=rep1&type=pdf>.]
- , and Coauthors, 2006: The 15-km version of the Canadian regional forecast system. *Atmos.–Ocean*, **44**, 133–149, doi:10.3137/ao.440202.
- Mainville, S., 2004: Heavy convective rain events over Quebec: A forecasting tool. Preprints, *22nd Conf. on Severe Local Storms*, Hyannis, MA, Amer. Meteor. Soc., P8.7. [Available online at <https://ams.confex.com/ams/pdfpapers/80902.pdf>.]
- Marshall, J. H., S. B. Trier, T. M. Weckwerth, and J. W. Wilson, 2011: Observations of elevated convection initiation leading to a surface-based squall line during 13 June IHOP\_2002. *Mon. Wea. Rev.*, **139**, 247–271, doi:10.1175/2010MWR3422.1.
- McTaggart-Cowan, R., and A. Zadra, 2015: Representing Richardson number hysteresis in the NWP boundary layer. *Mon. Wea. Rev.*, **143**, 1232–1258, doi:10.1175/MWR-D-14-00179.1.
- Mesinger, F., and Coauthors, 2006: North American Regional Reanalysis. *Bull. Amer. Meteor. Soc.*, **87**, 343–360, doi:10.1175/BAMS-87-3-343.
- Milrad, S. M., J. R. Gyakum, E. H. Atallah, and J. F. Smith, 2011: A diagnostic examination of the eastern Ontario and western Quebec wintertime convection event of 28 January 2010. *Wea. Forecasting*, **26**, 301–318, doi:10.1175/2010WAF2222432.1.
- , E. H. Atallah, J. R. Gyakum, and G. Dookhie, 2014: Synoptic typing and precursors of heavy warm-season precipitation events at Montreal, Quebec. *Wea. Forecasting*, **29**, 419–444, doi:10.1175/WAF-D-13-00030.1.
- Olson, D. A., N. W. Junker, and B. Korty, 1995: Evaluation of 33 years of quantitative precipitation forecasting at the NMC. *Wea. Forecasting*, **10**, 498–511, doi:10.1175/1520-0434(1995)010<0498:EOYOQP>2.0.CO;2.
- Ontario Climate Center, 2005: Data analysis and archive division. Environment Canada, accessed 4 February 2016. [Available online at [http://nadm.ontario.int.ec.gc.ca/Intranet/notices\\_e.cfm](http://nadm.ontario.int.ec.gc.ca/Intranet/notices_e.cfm).]
- Schumacher, R. S., and R. H. Johnson, 2005: Organization and environmental properties of extreme-rain-producing mesoscale convective systems. *Mon. Wea. Rev.*, **133**, 961–976, doi:10.1175/MWR2899.1.
- , and —, 2006: Characteristics of U.S. extreme rain events during 1999–2003. *Wea. Forecasting*, **21**, 69–85, doi:10.1175/WAF900.1.
- , and —, 2008: Mesoscale processes contributing to extreme rainfall in a midlatitude warm-season flash flood. *Mon. Wea. Rev.*, **136**, 3964–3986, doi:10.1175/2008MWR2471.1.
- , and —, 2009: Quasi-stationary, extreme-rain-producing convective systems associated with midlevel cyclonic circulations. *Wea. Forecasting*, **24**, 555–574, doi:10.1175/2008WAF2222173.1.
- Sukovich, E. M., F. M. Ralph, F. E. Barthold, D. W. Reynolds, and D. R. Novak, 2014: Extreme quantitative precipitation forecast performance at the Weather Prediction Center from 2001 to 2011. *Wea. Forecasting*, **29**, 894–911, doi:10.1175/WAF-D-13-00061.1.
- Sundqvist, H., 1978: A parameterization scheme for non-convective condensation including prediction of cloud water content. *Quart. J. Roy. Meteor. Soc.*, **104**, 677–690, doi:10.1002/qj.49710444110.
- , E. Berge, and J. E. Kristjánsson, 1989: Condensation and cloud parameterization studies with a mesoscale numerical weather prediction model. *Mon. Wea. Rev.*, **117**, 1641–1657, doi:10.1175/1520-0493(1989)117<1641:CACPSW>2.0.CO;2.
- University of Wyoming, 2014: Upper-air data. Department of Atmospheric Science, accessed 4 February 2016. [Available online at <http://weather.uwyo.edu/upperair/sounding.html>.]
- Weckwerth, T. M., and D. B. Parsons, 2006: A review of convection initiation and motivation for IHOP\_2002. *Mon. Wea. Rev.*, **134**, 5–22, doi:10.1175/MWR3067.1.
- Whiteman, C. D., X. Bian, and S. Zhong, 1997: Low-level jet climatology from enhanced rawinsonde observations at a site in the southern Great Plains. *J. Appl. Meteor.*, **36**, 1363–1376, doi:10.1175/1520-0450(1997)036<1363:LLJCFE>2.0.CO;2.
- Whittier, S. L., G. A. Hanson, and R. E. Bell, 2004: A conceptual model of warm season excessive rainfall used to warn for flooding of 12 June 2002 across northern Vermont. Preprints, *11th Conf. on Mountain Meteorology and the Annual Mesoscale Alpine Program (MAP)*, Bartlett, NH, Amer. Meteor. Soc., P9.1. [Available online at <https://ams.confex.com/ams/pdfpapers/76866.pdf>.]
- Wulfmeyer, V., and Coauthors, 2008: The convective and orographically induced precipitation study: A research and development project of the World Weather Research Program for improving quantitative precipitation forecasting in low-mountain regions. *Bull. Amer. Meteor. Soc.*, **89**, 1477–1486, doi:10.1175/2008BAMS2367.1.
- Xu, Q., and C. J. Qiu, 1997: A variational method for computing surface heat fluxes from ARM surface energy and radiation balance systems. *J. Appl. Meteor.*, **36**, 3–11, doi:10.1175/1520-0450(1997)036<0003:AVMFCS>2.0.CO;2.
- Zhang, D.-L., E.-Y. Hsie, and M. W. Moncrieff, 1988: A comparison of explicit and implicit predictions of convective and stratiform precipitating weather systems with a meso- $\beta$ -scale numerical model. *Quart. J. Roy. Meteor. Soc.*, **114**, 31–60, doi:10.1002/qj.49711447903.
- , J. S. Kain, J. M. Fritsch, and K. Gao, 1994: Comments on “Parameterization of convective precipitation in mesoscale numerical models: A critical review.” *Mon. Wea. Rev.*, **122**, 2222–2231, doi:10.1175/1520-0493(1994)122<2222:COOCPI>2.0.CO;2.
- , S. Zhang, and S. Weaver, 2006: Low-level jets over the mid-Atlantic states: Warm-season climatology and a case study. *J. Appl. Meteor. Climatol.*, **45**, 194–209, doi:10.1175/JAM2313.1.
- , Y. Lin, P. Zhao, X. Yu, S. Wang, H. Kang, and Y. Ding, 2013: The Beijing extreme rainfall of 21 July 2012: “Right results” but for wrong reasons. *Geophys. Res. Lett.*, **40**, 1426–1431, doi:10.1002/grl.50304.
- , L. Zhu, X. Zhang, and V. Tallapragada, 2015: Sensitivity of idealized hurricane intensity and structures under varying background flows and initial vortex intensities to different vertical resolutions in HWRF. *Mon. Wea. Rev.*, **143**, 914–932, doi:10.1175/MWR-D-14-00102.1.
- Zhang, M., and D.-L. Zhang, 2012: Subkilometer simulation of a torrential-rain-producing mesoscale convective system in east China. Part I: Model verification and convective organization. *Mon. Wea. Rev.*, **140**, 184–201, doi:10.1175/MWR-D-11-00029.1.